Early somatic mosaicism is a rare cause of long-QT syndrome

James Rush Priest[a,b,c], Charles Gawad[b,d,1], Kristopher M. Kahlig[e], Joseph K. Yu[f,g], Thomas O'Hara[f], Patrick M. Boyle[f,g], Sridharan Rajamani[e,2], Michael J. Clark[h], Sarah T. K. Garcia[h,3], Scott Ceresnak[a,b,c], Jason Harris[h], Sean Boyle[h], Frederick E. Dewey[a,i,4], Lindsey Malloy-Walton[a,b,c,5], Kyla Dunn[a,j], Megan Grove[a,i], Marco V. Perez[a,i], Norma F. Neff[k], Richard Chen[h], Katsuhide Maeda[a,l], Anne Dubin[a,b,c], Luiz Belardinelli[e], John West[h], Christian Antolik[m], Daniela Macaya[m], Thomas Quertermous[a,i], Natalia A. Trayanova[f,g], Stephen R. Quake[k,n,o,6], and Euan A. Ashley[a,b,i,6]

[a]Stanford Center for Inherited Cardiovascular Disease, Stanford University School of Medicine, Stanford, CA 94305; [b]Child Health Research Institute, Stanford University School of Medicine, Stanford, CA 94305; [c]Division of Pediatric Cardiology, Stanford University School of Medicine, Stanford, CA 94305; [d]Division of Pediatric Hematology-Oncology, Stanford University School of Medicine, Stanford, CA 94305; [e]Department of Biology, Cardiovascular Therapeutic Area, Gilead Sciences, Fremont, CA 94555; [f]Department of Biomedical Engineering, Johns Hopkins University, Baltimore, MD 21218; [g]Institute for Computational Medicine, Johns Hopkins University, Baltimore, MD 21218; [h]Personalis, Inc., Menlo Park, CA 94025; [i]Division of Cardiovascular Medicine, Stanford University School of Medicine, Stanford, CA 94305; [j]Lucile Packard Children's Hospital Heart Center, Palo Alto, CA 94304; [k]Department of Bioengineering, Stanford University School of Medicine, Stanford, CA 94305; [l]Division of Cardiothoracic Surgery, Stanford University School of Medicine, Stanford, CA 94305; [m]Cardiogenetic Testing Services, GeneDx, Gaithersburg, MD 20877; [n]Department of Applied Physics, Stanford University, Stanford, CA 94305; and [o]Howard Hughes Medical Research Institute, Stanford University School of Medicine, Stanford, CA 94305

Contributed by Stephen R. Quake, August 19, 2016 (sent for review May 5, 2016; reviewed by Leslie Biesecker and Christopher Semsarian)

Somatic mosaicism, the occurrence and propagation of genetic variation in cell lineages after fertilization, is increasingly recognized to play a causal role in a variety of human diseases. We investigated the case of life-threatening arrhythmia in a 10-day-old infant with long QT syndrome (LQTS). Rapid genome sequencing suggested a variant in the sodium channel $Na_V1.5$ encoded by *SCN5A*, NM_000335:c.5284G > T predicting p.(V1762L), but read depth was insufficient to be diagnostic. Exome sequencing of the trio confirmed read ratios inconsistent with Mendelian inheritance only in the proband. Genotyping of single circulating leukocytes demonstrated the mutation in the genomes of 8% of patient cells, and RNA sequencing of cardiac tissue from the infant confirmed the expression of the mutant allele at mosaic ratios. Heterologous expression of the mutant channel revealed significantly delayed sodium current with a dominant negative effect. To investigate the mechanism by which mosaicism might cause arrhythmia, we built a finite element simulation model incorporating Purkinje fiber activation. This model confirmed the pathogenic consequences of cardiac cellular mosaicism and, under the presenting conditions of this case, recapitulated 2:1 AV block and arrhythmia. To investigate the extent to which mosaicism might explain undiagnosed arrhythmia, we studied 7,500 affected probands undergoing commercial gene-panel testing. Four individuals with pathogenic variants arising from early somatic mutation events were found. Here we establish cardiac mosaicism as a causal mechanism for LQTS and present methods by which the general phenomenon, likely to be relevant for all genetic diseases, can be detected through single-cell analysis and next-generation sequencing.

mosaicism | arrhythmia | genomics | computational modeling | single cell

There is growing recognition that somatic mosaicism, i.e., genetic variation within an individual that arises from errors in DNA replication during early development, may play a role in a variety of human diseases other than cancer (1). However, the extent to which cellular heterogeneity contributes to disease is minimally understood. One report suggests that 6.5% of de novo mutations presumed to be germline in origin may instead have arisen from postzygotic mosaic mutation events (2), and recent genetic investigations directly interrogating diseased tissues in brain malformations, breast cancer, and atrial fibrillation have revealed postzygotic causal mutations absent from germline DNA (3–6). Pathogenic mosaic structural variation is also detectable in children with neurodevelopmental disorders (7). However, a consequential category of genetic variation has not been surveyed systematically in clinical or research studies of other human diseases.

The pathophysiological basis of long-QT syndrome (LQTS) is prolongation of cardiac ventricular repolarization by acquired factors such as drug exposure or genetic variation in the proteins controlling transmembrane ion-concentration gradients (8, 9); parental gonadal mosaicism is an infrequently described phenomenon in LQTS (10–12). Knowledge of the molecular subtyping of disease in LQTS has provided a foundation for genotype-specific risk stratification and treatment strategies (8, 9,

Significance

Most genetic studies and clinical genetic testing do not look for the possibility of mosaic variation. The genetic form of long-QT syndrome (LQTS) can result in life-threatening arrhythmias, but 30% of patients do not have a genetic diagnosis. We performed deep characterization of a mosaic variant in an infant with perinatal LQTS and developed a computational model showing how abnormal cellular repolarization in only 8% of heart cells may cause arrhythmia. Finally we looked at the prevalence of mosaicism among patients with LQTS; in a population of 7,500 individuals we found evidence of pathogenic early somatic mosaicism in approximately 0.17% of LQTS patients without a genetic diagnosis. Together these data establish an unreported mechanism for LQTS and other genetic arrhythmias.

Author contributions: J.R.P., K.M.K., T.O., S.R., S.C., R.C., K.M., A.D., L.B., J.W., D.M., T.Q., and E.A.A. designed research; J.R.P., C.G., K.M.K., J.K.Y., P.M.B., L.M.-W., K.D., M.G., M.V.P., and C.A. performed research; J.K.Y., T.O., P.M.B., F.E.D., N.F.N., D.M., N.A.T., and S.R.Q. contributed new reagents/analytic tools; J.R.P., C.G., K.M.K., J.K.Y., P.M.B., M.J.C., S.T.K.G., J.H., S.B., and J.W. analyzed data; and J.R.P., K.M.K., J.K.Y., T.Q., and E.A.A. wrote the paper.

Reviewers: L.B., NIH; and C.S., University of Sydney.

Conflict of interest statement: At the time of this work K.M.K., S.R., and L.B. were employed by Gilead Sciences. M.J.C., S.T.K.G., S.B., J.W., and R.C. were employed by Personalis, Inc. J.W. and E.A.A. are founders of Personalis, Inc. which offers clinical genetic testing but does not offer Clinical Laboratory Improvement Amendments (CLIA)-certified rapid-turnaround whole-genome sequencing. N.A.T. is a co-founder of CardioSolv LLC.

Freely available online through the PNAS open access option.

[1]Present address: St. Jude Children's Research Hospital, Memphis, TN 38105.

[2]Present address: Amgen, Inc., South San Francisco, CA 94080.

[3]Present address: 10X Genomics, Pleasanton, CA 94556.

[4]Present address: Regeneron Pharmaceuticals, Tarrytown, NY 10591.

[5]Mercy Children's Hospital, Kansas City, MO 64108.

[6]To whom correspondence may be addressed. Email: euan@stanford.edu or quake@stanford.edu.

This article contains supporting information online at www.pnas.org/lookup/suppl/doi:10.1073/pnas.1607187113/-/DCSupplemental.

13, 14). However, nearly 30% of probands remain undiagnosed using standard commercial gene-panel testing, suggesting there is unrecognized genetic variation (genic, regulatory, or otherwise) yet to be associated with disease (15).

In its most severe form, LQTS may occur in the neonatal period with bradycardia and functional 2:1 AV block that occur secondary to a severely prolonged ventricular refractory period greater than the short R–R interval characteristic of a normal heart rate in infancy (16). Patients of all ages presenting with LQTS are predisposed to torsades de pointes (TdP), a life-threatening cardiac arrhythmia, with patients presenting in infancy showing particularly poor outcomes (13, 16–18). In this study, we applied rapid-turnaround whole-genome sequencing (WGS) on day of life (DOL) 3 in a premature infant with perinatal LQTS and life-threatening arrhythmia and investigated the contribution of a discovered mosaic variant to abnormal cardiac electrophysiology at the molecular and tissue levels. Additionally we surveyed 7,500 individuals already tested for genetic arrhythmias, allowing us to estimate the prevalence of mosaicism in an unbiased population sample.

Results

Deep Sequencing Identifies Mosaic Variation in *SCN5A* in an Infant with a Prolonged QT Interval and Arrhythmia. A near-term 2.5-kg female infant of Asian ancestry with prenatally diagnosed 2:1 AV block was delivered by caesarean section at 36-wk gestation. At 1 h of life the infant developed intermittent 2:1 AV block with multiple episodes of TdP with a corrected QT interval (QTc) of 542 ms (Fig. 1), which were relieved by placement of a dual-chamber epicardial implantable cardioverter/defibrillator (ICD) accompanied by a bilateral stellate ganglionectomy. A standard commercially available genetic panel for LQTS was sent on DOL 1 (13, 17), and WGS was performed on DOL 3. At 6 mo of age the patient developed dilated cardiomyopathy and subsequently received an orthotopic heart transplant.

WGS yielded a 39.76 mean read depth, and coverage across the coding regions of known LQTS and dilated cardiomyopathy (DCM) genes was 99.93% at 10× or greater (Table S1). The rapid RTG pipeline detected a mutation in the 28th exon of the voltage-gated sodium channel $Na_V1.5$ encoded by *SCN5A* NM_000335: c.5284G > T, which predicts p.(V1762L) within the alpha subunit of $Na_V1.5$, which was not present in the two additional call sets originating from Burrows–Wheeler Aligner (BWA)/Genome Analysis Toolkit (GATK) or Issac (Issac Genome Alignment Software and Variant Caller) pipelines. All three pipelines detected rs41261344, a polymorphism in *SCN5A* common in Han Chinese NM_000335: c.3575G > A, which predicts p.R1193Q (22).

Given the discrepant results between the WGS pipelines, we performed Sanger sequencing of PCR amplicons derived from proband blood and saliva that did not show the T allele coding for the p.(V1762L) mutation. Inspection of raw reads and Sanger electropherograms suggested a low abundance of the mutant T allele (eight reads) compared with the G allele (26 reads) (Fig. 2). Because the reads supporting the 23.5% mutant allele fraction displayed good sequence quality and were without evidence of strand bias, and because manual inspection and remapping of the mutant reads confirmed their optimal mapping to *SCN5A* despite the paralogous evolutionary relationship of *SCN5A* to other ion channels, we elected to perform exome sequencing of the family trio using a second proband blood sample and saliva samples from each parent. Deep augmented exome sequencing confirmed the presence of the T allele uniquely in the proband sample at a ratio of 17 mutant T allele reads to 210 G allele reads, a mutant allele fraction of 7.5%. Deleterious variation in the *SCN5A* gene is associated with a spectrum of interrelated cardiac disorders including LQTS and DCM (23, 24), and no additional Mendelian or somatic variants

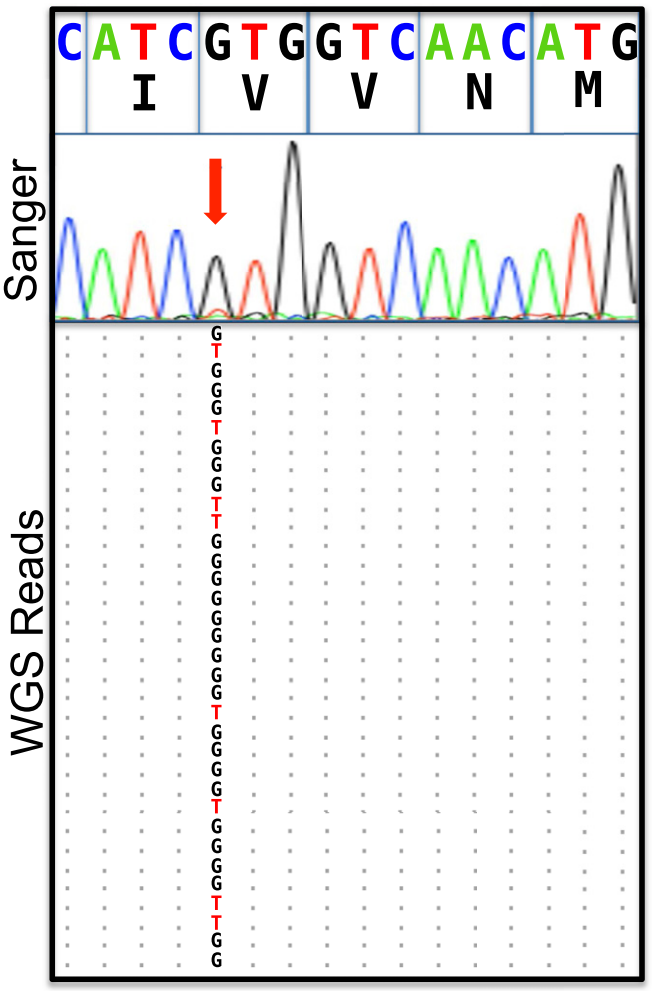

Fig. 2. Mosaicism in the *SCN5A* locus is suggested by rapid genome sequencing and confirmed by augmented deep-exome sequencing. Alignments of next-generation sequencing reads from the *SCN5A* gene on chromosome 3 derived from rapid genome sequencing, with a cartoon alignment of the reverse complement of next-generation sequencing reads covering base pairs 38, 592, 565–38, 592, and 580 and a Sanger electropherogram suggestive of mosaicism indicated by the red arrow. Coordinates are from the hg19 assembly of the human genome. The allelic balance by genome sequencing (26 G, 8 T) is unlikely to arise from a 50:50 balance at a heterozygous locus (one-sided binomial test, $P = 0.001$), and the allelic balance observed by exome sequencing (210 G, 17 T) effectively rules out a variant with Mendelian inheritance at this position.

Fig. 1. Representative electrocardiograms from DOL 1 show a prolonged QT interval and 2:1 atrioventricular block. (*A*) A rhythm strip from lead II of a 12-lead ECG before treatment shows a prolonged QTc of 542 ms estimated by Bazett's formula. (*B*) A rhythm strip showing 2:1 atrioventricular block secondary to prolongation of the QT interval. (*C*) A rhythm strip demonstrating polymorphic ventricular tachycardia.

causative for LQTS or cardiomyopathy were discovered on exome sequencing or WGS (*SI Methods* and Table S2 and Table S3).

The V1762L Channel Displays Profoundly Abnormal Late Sodium Current with a Dominant Effect. The valine residue 1762 occurs within a highly conserved transmembrane helix of $Na_V1.5$. In a previously reported case of perinatal LQTS, a methionine mutation caused by a single-nucleotide variant at the identical genomic position (rs199473631, c.5284G > A predicting p.V1762M) showed a late sustained sodium current (I_{Na}) and rapid recovery from inactivation compared with the WT channel (25). In representative whole-cell I_{Na} recorded from human tsA201 cells, the V1762L mutant channel exhibited delayed I_{Na} inactivation compared with the WT channel and resulted in the expression of a large late I_{Na} (Fig. 3*A*). Full inactivation of the I_{Na} within a 220-ms interval, as seen in the WT and R1193Q channels, was not observed in the V1762L channel (Fig. 3*B*), and the late I_{Na} was significantly greater than in WT channels [0.92 ± 0.06% (SEM) of peak I_{Na}, $n = 6$ versus 0.03 ± 0.02% of peak I_{Na}; $n = 6$, respectively; $P < 0.001$] (Fig. 3*C*). The persistent late I_{Na} seen in the V1762L construct was unchanged when cotransfected with either WT *SCN5A* or the common R1193Q variant channel, suggesting a dominant effect of V1762L on the action potential (Fig. 3*C*). The abnormal inactivation observed for the V1762L construct is expected to be particularly severe because it combines both a slowed time course of inactivation and large non-inactivating I_{Na}. The R1193Q variant did not exhibit a functional defect compared with WT channels, as is consistent with its predicted role as a benign or weakly modifying common variant. The profoundly abnormal late I_{Na} displayed by the V1762L construct in vitro is strongly consistent with the pathogenic mechanism of LQTS.

Mosaicism of the p.(V1762L) Variant Is Present in Multiple Tissues and Is Expressed in Cardiomyocytes. To verify the mosaicism of p.(V1762L) at the single-cell level, individual peripheral blood mononuclear cells from a third blood draw were isolated, lysed, and genotyped with a custom assay following whole-genome amplification. We detected the p.(V1762L) variant in amplified DNA from 3 of 36 isolated cells (Fig. 4*A*). Direct Sanger sequencing of cloned PCR products derived from these single cells

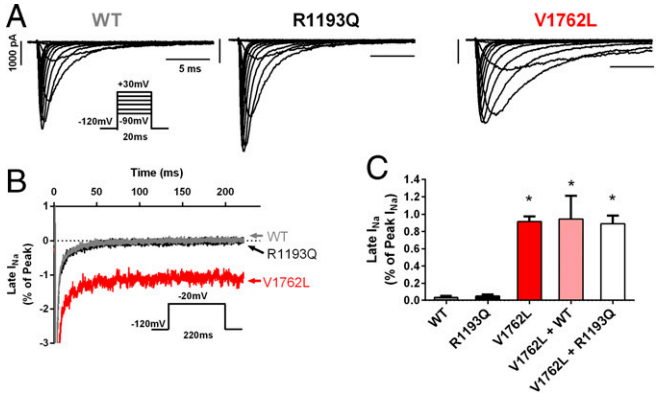

Fig. 3. p.(V1762L) mutant channel exhibits defective I_{Na} inactivation consistent with a LQT3 phenotype. (*A*) Representative whole-cell I_{Na} traces recorded from cells expressing WT (*Left*), the common variant R1193Q (*Center*), or the mutant V1762L (*Right*). Note the delayed I_{Na} inactivation in the V1762L channel. (*B*) Extended voltage-step protocols reveal a late (sustained) I_{Na} conducted by V1762L (red trace), which was absent in both the WT and R1193Q channels. The dotted line indicates zero current. (*C*) The average late I_{Na} conducted by V1762L was significantly greater than that in WT (0.92 ± 0.06% of peak I_{Na}, $n = 6$, versus 0.03 ± 0.02% of peak I_{Na}, $n = 6$, respectively; $^*P < 0.001$). No late I_{Na} was seen with the R1193Q mutation. The V1762L construct exerted a strongly dominant effect when cotransfected with either the WT channel (V1762L + WT) or R1193Q mutant (V1762L + R1193Q), maintaining a profoundly abnormal late I_{Na}.

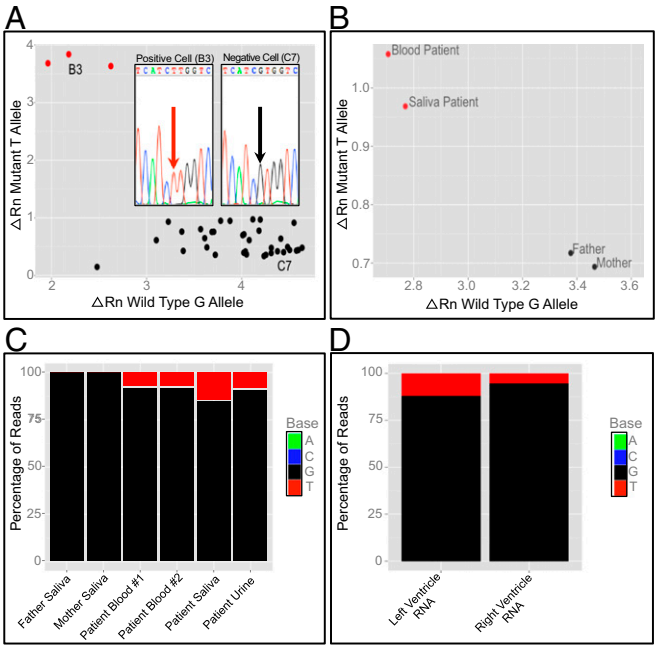

Fig. 4. Single-cell genotyping and targeted resequencing suggest that a mutation event causing mosaicism occurred before gastrulation. (*A*) qPCR genotyping of amplified DNA from 36 individual peripheral blood mononuclear cells identifies a subpopulation of three cells (red) that contain the T allele encoding the p.(V1762L) variant. A positive cell (B3) and negative cell (C7) are identified for the purposes of Sanger sequencing of cloned PCR products, respectively confirming the presence and absence of the mutant T allele (*Inset*). For each axis, the ΔRn value represents the magnitude of the signal generated from annealing of the allele-specific fluorescent probe to either the mutant or the WT allele relative to a signal generated from a passive reference dye during PCR amplification. (*B*) qPCR genotyping of DNA from proband blood, proband saliva, and parental saliva demonstrates the presence of the T allele only in proband samples. (*C*) Resequencing of PCR amplicons from four separate proband and both parental samples demonstrates that the frequency of the mutation is similar in proband blood (7.9%), urine (9.1%), and saliva (14.8%) samples, but the mutation is absent in both parental samples. (*D*) RNA sequencing of patient heart samples from the left and right ventricles identifies *SCN5A* reads containing the mutant allele.

confirmed the genotyping assay (Fig. 4*A*, *Inset*). We repeated the TaqMan genotyping assay in standard fashion on proband and parental DNA and again detected the T allele uniquely in the proband sample only (Fig. 4*B*).

The timing of a mutation event during early embryogenesis would significantly affect the abundance and tissue lineages of clonal subpopulations of cells containing a variant. To determine when the mutation event occurred and to quantify the extent of mosaicism directly, we performed next-generation sequencing of PCR amplicons derived from proband DNA sources representing cellular lineages originating from the three primordial germ layers: blood (mesoderm), urine (endoderm), and saliva (endoderm and ectoderm). Tissue representing all three lineages revealed that the T allele comprised 7.9–14.8% of all high-quality reads and was absent from parental samples (Fig. 4*C*); a quantitative PCR (qPCR) genotyping assay confirmed the presence of the T allele uniquely in all proband DNA samples (Fig. S1). The presence of the allele in all primordial germ layers suggested that the mutation occurred during the cell divisions expanding the blastocyst before gastrulation and that the presence of the mutation was not limited to hematopoietic derivatives. To confirm this finding, two separate ventricular myocardial samples were obtained at the time of heart transplant; RNA sequencing revealed expression of the mutant allele in 5.4–11.8% of all *SCN5A* transcripts (Fig. 4*D*).

A Computational Model of Cardiac Electrophysiology Links Mosaicism in the Conduction Tissue to Arrhythmia. To explore the mechanism by which a small proportion of cells with persistent late I_{Na} in mosaic expression patterns could give rise to the observed clinical phenotype (2:1 block and/or proarrhythmic activation sequence), we performed simulations using a biophysically detailed 3D model of the ventricles including the Purkinje system. We considered two possible patterns of mosaicism (Fig. S2): diffuse and clustered. Mosaicism in ventricular cardiomyocytes alone did not recapitulate the 2:1 block or arrhythmia-prone phenotype observed in our patient. However, when mosaicism also was incorporated in the Purkinje fibers, a subset of pacing sequences resulted in 2:1 block (i.e., every other His bundle stimulus produced no ventricular activation) (Fig. 5*A*). With the three models of cellular distribution (WT, diffuse mosaic, clustered mosaic), the simulations showed six distinct ventricular activation regimes resulting from the 81 different pacing sequences tested (Fig. 5*B*). Highly arrhythmogenic behavior (i.e., 2:1 block with or without left bundle branch block, LBBB) was observed for the majority of pacing sequences in both the diffuse mosaic model (in which arrhythmogenic behavior was observed for 79% of pacing configurations) and the clustered mosaic model (in which arrhythmogenic behavior was observed in 80% of pacing configurations) but never in the WT model (Fig. 5*C*). Notably, pacing sequences with coupling intervals within the physiological range for resting neonatal heart rates (400- to 600-ms cycle length; black boxes in Fig. 5*C*) led to 2:1 block in 48% of the simulations conducted with the diffuse mosaic model and in 52% of the simulations conducted with the clustered mosaic model. For the same pacing sequences, no instances of conduction block or LBBB were observed in the WT model.

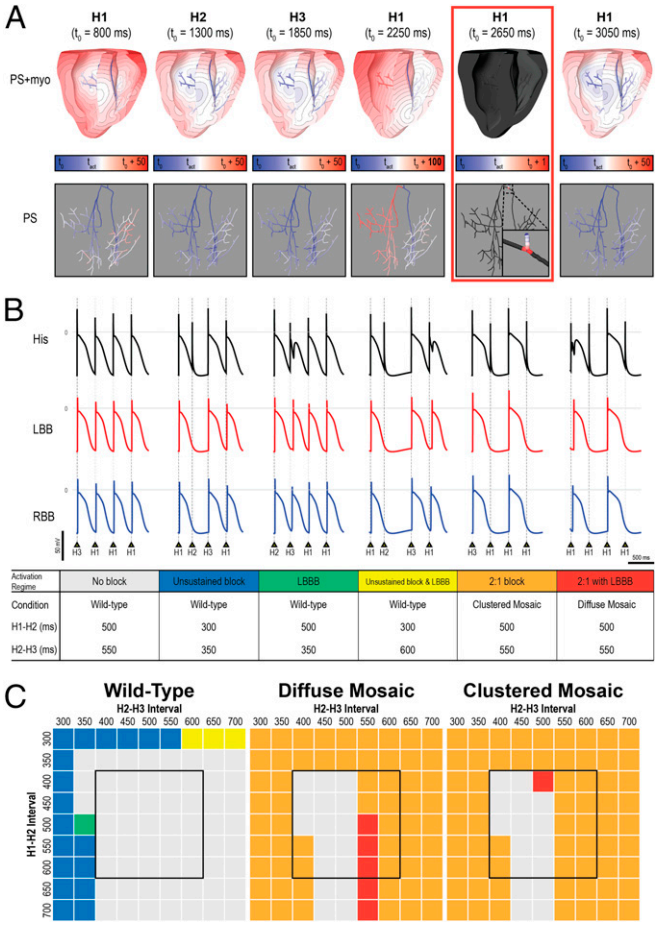

Fig. 5. Mosaic expression of the V1762L mutation in a 3D computational model of fetal ventricles and the Purkinje system leads to 2:1 block and LBBB. (*A*) Activation maps for six consecutive His bundle stimuli (delivered at t_0 shown for each map) for the diffuse mosaic model; cutaway (*Upper*) and Purkinje-only (*Lower*) views are shown. Activation time scales are relative to t_0 and vary for the different beats. Panel 4 shows an LBBB excitation sequence; excitation of the left side of the Purkinje system was caused by retrograde conduction from ventricular tissue. Panel 5 (red box) shows a conduction block in the His bundle, which initiated the 2:1 block activation regime. (*B*) Representative action potential sequences from the His bundle and the left/right bundle branches (LBB and RBB) for the six distinct activation regimes observed in response to different pacing protocol configurations: no blocked sinus beats; single blocked beat (i.e., no 2:1 block), without or with LBBB; LBBB with no blocked beats; and 2:1 block without or with LBBB. In cases with LBBB, action potential onset in the LBB was delayed (rightward shift), and late excitation of the His bundle caused by retrograde conduction was observed as a bump during repolarization. Fig. S2*B* shows the exact Purkinje locations from which action potential traces were extracted. (*C*) Summary of outcomes for all 243 unique simulations (81 pacing sequences in three models); the color of each entry corresponds to one of the activation regimes in *B*. Black boxes highlight the range of coupling intervals associated with the normal resting sinus rate for human infants.

Early Somatic Mosaicism Is Detectable in Patient Populations with LQTS. Having established a plausible mechanism by which a percentage of cells with abnormal late I_{Na} might significantly alter the cardiac action potential, we sought to determine more broadly the prevalence of early somatic mosaicism among individuals with a genetic arrhythmia. We looked for evidence of mosaicism among a group of 7,500 samples submitted to a commercial testing company for one or more next-generation sequencing panel tests for genetic arrhythmias (up to 30 genes tested). Among the 7,500 individuals, four affected individuals, i.e., 0.05% of all cases, displayed apparent mosaicism within a gene causing LQTS. In studies of panel genetic testing, a causal genetic variant is typically identified in ~70% of individuals undergoing genetic testing for genetic arrhythmia, leaving 30% without a diagnosis (15); our results suggest a prevalence of mosaicism in ~0.17% of undiagnosed cases. Of the four individuals with mosaic variants, one was an infant, and none displayed another Mendelian LQTS variant that explained the arrhythmia phenotype. Three additional individuals with pathogenic mosaic variants in LQTS genes appeared to be founders, because they were identified when undergoing family testing for an affected relative with a Mendelian LQTS variant. These data confirm that early somatic mutation events occurring before gastrulation are a relatively uncommon occurrence and that early mosaicism represents a rare but recurrent cause of genetic arrhythmias.

Discussion

Although LQTS has long been considered a Mendelian disorder, deep characterization of a single patient and population-scale data suggest that early somatic mosaicism is a rare cause of human arrhythmias. Here we present an integrative computational simulation of the cardiac action potential that illustrates a pathogenic mechanism by which mosaicism within the specialized conducting tissue alters the predisposition to arrhythmia; this mechanism is missing from previous reports of other arrhythmias caused by somatic mosaicism (3, 6). Together these data link a small amount of cellular heterogeneity to disordered cardiac rhythm.

To explore the fundamental mechanism by which a profound derangement in a small percentage of cells within the heart might cause a severe phenotype, we developed an organ-level computational simulation of the cardiac action potential integrating mosaicism at the cellular level with generic representations of an infant-sized heart. Given the absence of primary electrophysiological data from neonatal human cardiomyocytes, the parameters

for ion flux do not account for immature calcium handling unique to newborn cardiac physiology.

Nevertheless, the finite model simulation suggested that somatic mosaicism within the Purkinje system can lead to abnormal electrophysiological propagation consistent with LQTS, offering a potential explanation for the development of an arrhythmia-prone substrate. Previous computational and experimental work has also suggested that the Purkinje system may play a primary role in arrhythmias related to LQTS (26, 27). Our simulations demonstrated significantly prolonged action potential duration resulting from increased late I_{Na} (Fig. S3), which increased the propensity for block occurring in the Purkinje system. Both the diffuse and clustered mosaic models showed 2:1 AV block at physiological heart rates observed in the infant and are consistent with the clinical observation of immediate improvement in cardiac conduction parameters with dual-chamber pacing. When combined with the clinical and genetic observations, the simulation data provide additional support for the pathological role of the Purkinje system in arrhythmias and suggest a mechanism by which even a small amount cardiac mosaicism may result in clinically significant arrhythmia.

The association of early somatic mosaicism with LQTS adds to the developing framework describing the contribution of postzygotic mutations to human genetic variation. In a recently proposed model of human germline mutation rates derived from exome sequencing of a large autozygous population, the contribution of postzygotic mutations to germline mutation rates was below the threshold of detection (28). In an alternative empirical approach tracing the origin of de novo mutations in 50 trios undergoing WGS, only 0.1% of de novo mutations were derived from low-level parental gonadal mosaicism (2). However, in the same study, 6.5% of presumed de novo mutations displayed allelic imbalance, suggesting a postzygotic mutation event (2). Modeling of postzygotic mutation rates in a third family-based study suggests different rates over the course of embryonic development and postnatal life, with mutation rates peaking during the rapid cell divisions underlying organogenesis following gastrulation (29). Although the prevalence of mosaic variation in our population-based sample of 7,500 individuals appears relatively low, at 0.05%, this conservative estimate accounts only for the detection of early mutation events occurring in all tissues throughout the body (and thus detectable in blood or saliva) during approximately the first four postzygotic cell divisions. To ascertain the possibility of disease-causing tissue-specific mutation events occurring later during development, when mutation rates may be higher (29), systematic surveys of DNA obtained directly from diseased tissues or cell-free DNA are necessary.

Conspicuously, the commercial gene-panel test for this patient returned a negative result, and somatic mutations of relatively low abundance are not universally reported by commercial gene-panel testing. For detection of early mosaic mutation events (occurring during the 10 cell divisions after fertilization before gastrulation), the count of individual molecules derived from next-generation sequencing-by-synthesis chemistries enables a simple likelihood estimation of the underlying allelic balance. The observation of exactly 8 of 34 (23.5%) variants containing reads from a heterozygous locus (Fig. 2) was strongly suggestive of an underlying imbalance of alleles (Fig. S4). When tuned to detect mosaicism, simple analytical schema based on the binomial distribution are adaptable to sequencing reads from gene-panel, exome, or whole-genome tests to detect mutations present in all tissues arising from early somatic mutation events. Although secondary confirmation has previously been the gold standard for confirming mosaicism, next-generation sequencing technologies are fundamentally more sensitive than Sanger sequencing in the detection of low-level mosaicism (2, 30). The accuracy of likelihood estimates and thus the sensitivity for detecting mosaicism in next-generation sequencing are related directly to the number of reads, thus strongly supporting the use of higher read-depth sequencing for clinical and research studies focused on detecting novel variants.

The discovery of a mosaic *SCN5A* variant affirms that rapid genetic diagnosis of neonatal disease by WGS may offer an alternative to standard gene-panel testing (31–33). In our view, rapid comprehensive genetic testing (WGS or whole-exome sequencing) should be used as a primary diagnostic inquiry in infants with life-threatening illness of unclear or suspected genetic etiology. Although the sensitivity and specificity for Mendelian variation have been the focus of applied and technical reports of clinical WGS (31, 34, 35), the discrepant results of the three WGS pipelines suggest that the predictive characteristics of WGS for somatic mosaicism are dependent on the informatics strategies used. Guidelines for detecting, confirming, and reporting mosaic variants in genes causing Mendelian disease in genetic diagnostics have yet to be addressed by professional organizations (36–38).

In summary, for a single case of perinatal LQTS we conclude that a mosaic variant, p.(V1762L), is pathogenic, demonstrating abnormal late I_{Na}, low-level mosaicism in multiple tissues throughout the body, and expression in cardiac tissue. A computational model of disease suggested a clear mechanism of pathogenesis linked to mosaicism in the conduction tissue. Finally, we show that early somatic mosaicism displays a low-level prevalence at a population scale. These data illustrate that somatic mosaicism represents a mechanism by which causal variation is missed in studies of genetic disease such as LQTS. However, our estimates of the prevalence of somatic mosaicism are limited to ascertaining early mutation events detectable in blood or saliva; events occurring later in development that are detectable only within cardiac tissue may constitute additional, as yet unmeasured genetic risk for LQTS. More broadly, our findings exemplify how careful scrutiny of WGS data and computational modeling of a single patient may serve as the foundation for new insights into human pathophysiology; such deep explorations will form the heart of precision medicine as applied to cardiovascular disease (39).

Methods

Genome sequencing was performed by Illumina Corporation, and exome sequencing, targeted sequencing, and RNA sequencing were performed by Personalis, Inc. Cellular patch-clamp measurements of I_{Na} were performed in human tsA201 cells using an Axoclamp 200B amplifier, Digidata 1400 digitizer, and pClamp 10 software (Molecular Devices). Peripheral blood mononuclear cells were isolated and loaded onto a prepared C1 small whole-genome amplification (WGA) microfluidic chip (Fluidigm Corporation), which performed lysis and whole-genome amplification on all viable cells. Computational simulations were conducted in a biophysically detailed 3D computational model of the heart calibrated to represent the size and geometry of the neonatal human ventricles, including representations of the Purkinje system and the muscle fiber orientation, using a validated software platform (19–21). Additional details may be found in *SI Methods* and Figs. S1–S7.

All research presented here was conducted under the guidelines of the Declaration of Helsinki and was approved by the Stanford Administrative Panels for the Protection of Human Subjects. On behalf of themselves and their infant daughter, the parents provided written informed consent for participation in this study. The parents also received genetic counseling from genetic counselors and physicians regarding the risks and benefits of genome sequencing. In the written consent process (as a checkbox on the consent form) and verbally, the parents expressed a preference to abstain from the report of incidentally discovered genetic information regarding long-term risks of other diseases such as cancer, neurodegenerative disorders, or cardiovascular disease.

ACKNOWLEDGMENTS. We thank Tina Hambuch; Marc Laurent at Illumina Corporation; Brian Hillbush and Len Trigg at Real Time Genomics; Christian Haudenschild at Personalis; and Justin Zook and Robert Dickson for discussions of the manuscript. This work was supported by NIH Grants DP2-OD006511 and U01-HG007708-03 (to E.A.A.) and R01 HL103428 and DP1 HL123271 (to N.A.T.). J.R.P. was supported by NIH Grants K12-HD000850 and K99-HL130523, and F.E.D. and M.V.P. were supported by NIH Grant T32-HL094274.

1. Biesecker LG, Spinner NB (2013) A genomic view of mosaicism and human disease. *Nat Rev Genet* 14(5):307–320.
2. Acuna-Hidalgo R, et al. (2015) Post-zygotic point mutations are an underrecognized source of de novo genomic variation. *Am J Hum Genet* 97(1):67–74.
3. Thibodeau IL, et al. (2010) Paradigm of genetic mosaicism and lone atrial fibrillation: Physiological characterization of a connexin 43-deletion mutant identified from atrial tissue. *Circulation* 122(3):236–244.
4. Ruark E, et al.; Breast and Ovarian Cancer Susceptibility Collaboration; Wellcome Trust Case Control Consortium (2013) Mosaic PPM1D mutations are associated with predisposition to breast and ovarian cancer. *Nature* 493(7432):406–410.
5. Jamuar SS, et al. (2014) Somatic mutations in cerebral cortical malformations. *N Engl J Med* 371(8):733–743.
6. Gollob MH, et al. (2006) Somatic mutations in the connexin 40 gene (GJA5) in atrial fibrillation. *N Engl J Med* 354(25):2677–2688.
7. King DA, et al.; Deciphering Developmental Disorders Study (2015) Mosaic structural variation in children with developmental disorders. *Hum Mol Genet* 24(10):2733–2745.
8. Lu JT, Kass RS (2010) Recent progress in congenital long QT syndrome. *Curr Opin Cardiol* 25(3):216–221.
9. Giudicessi JR, Ackerman MJ (2013) Genotype- and phenotype-guided management of congenital long QT syndrome. *Curr Probl Cardiol* 38(10):417–455.
10. Dufendach KA, Giudicessi JR, Boczek NJ, Ackerman MJ (2013) Maternal mosaicism confounds the neonatal diagnosis of type 1 Timothy syndrome. *Pediatrics* 131(6):e1991–e1995.
11. Miller TE, et al. (2004) Recurrent third-trimester fetal loss and maternal mosaicism for long-QT syndrome. *Circulation* 109(24):3029–3034.
12. Etheridge SP, et al. (2011) Somatic mosaicism contributes to phenotypic variation in Timothy syndrome. *Am J Med Genet A* 155A(10):2578–2583.
13. Cuneo BF, et al. (2013) Arrhythmia phenotype during fetal life suggests long-QT syndrome genotype: Risk stratification of perinatal long-QT syndrome. *Circ Arrhythm Electrophysiol* 6(5):946–951.
14. Priori SG, et al. (2013) HRS/EHRA/APHRS expert consensus statement on the diagnosis and management of patients with inherited primary arrhythmia syndromes: Document endorsed by HRS, EHRA, and APHRS in May 2013 and by ACCF, AHA, PACES, and AEPC in June 2013. *Heart Rhythm* 10(12):1932–1963.
15. Lieve KV, et al. (2013) Results of genetic testing in 855 consecutive unrelated patients referred for long QT syndrome in a clinical laboratory. *Genet Test Mol Biomarkers* 17(7):553–561.
16. Mitchell JL, et al. (2012) Fetal heart rate predictors of long QT syndrome. *Circulation* 126(23):2688–2695.
17. Aziz PF, et al. (2010) Congenital long QT syndrome and 2:1 atrioventricular block: An optimistic outcome in the current era. *Heart Rhythm* 7(6):781–785.
18. Crotti L, et al. (2013) Long QT syndrome-associated mutations in intrauterine fetal death. *JAMA* 309(14):1473–1482.
19. Boyle PM, Veenhuyzen GD, Vigmond EJ (2013) Fusion during entrainment of orthodromic reciprocating tachycardia is enhanced for basal pacing sites but diminished when pacing near Purkinje system end points. *Heart Rhythm* 10(3):444–451.
20. Rodríguez B, Li L, Eason JC, Efimov IR, Trayanova NA (2005) Differences between left and right ventricular chamber geometry affect cardiac vulnerability to electric shocks. *Circ Res* 97(2):168–175.
21. Boyle PM, Massé S, Nanthakumar K, Vigmond EJ (2013) Transmural IK(ATP) heterogeneity as a determinant of activation rate gradient during early ventricular fibrillation: Mechanistic insights from rabbit ventricular models. *Heart Rhythm* 10(11):1710–1717.
22. Hwang HW, et al. (2005) R1193Q of SCN5A, a Brugada and long QT mutation, is a common polymorphism in Han Chinese. *J Med Genet* 42(2):e7–author reply e8.
23. Shi R, et al. (2008) The cardiac sodium channel mutation delQKP 1507-1509 is associated with the expanding phenotypic spectrum of LQT3, conduction disorder, dilated cardiomyopathy, and high incidence of youth sudden death. *Europace* 10(11):1329–1335.
24. Chockalingam P, Wilde A (2012) The multifaceted cardiac sodium channel and its clinical implications. *Heart* 98(17):1318–1324.
25. Chang C-C, et al. (2004) A novel SCN5A mutation manifests as a malignant form of long QT syndrome with perinatal onset of tachycardia/bradycardia. *Cardiovasc Res* 64(2):268–278.
26. Iyer V, Sampson KJ, Kass RS (2014) Modeling tissue- and mutation- specific electrophysiological effects in the long QT syndrome: Role of the Purkinje fiber. *PLoS One* 9(6):e97720.
27. Ben Caref E, Boutjdir M, Himel HD, El-Sherif N (2008) Role of subendocardial Purkinje network in triggering torsade de pointes arrhythmia in experimental long QT syndrome. *Europace* 10(10):1218–1223.
28. Narasimhan VM, et al. (2016) A direct multi-generational estimate of the human mutation rate from autozygous segments seen in thousands of parentally related individuals. bioRxiv:059436.
29. Rahbari R, et al.; UK10K Consortium (2016) Timing, rates and spectra of human germline mutation. *Nat Genet* 48(2):126–133.
30. Beck TF, Mullikin JC, Biesecker LG; NISC Comparative Sequencing Program (2016) Systematic evaluation of Sanger validation of next-generation sequencing variants. *Clin Chem* 62(4):647–654.
31. Priest JR, et al. (2014) Molecular diagnosis of long QT syndrome at 10 days of life by rapid whole genome sequencing. *Heart Rhythm* 11(10):1707–1713.
32. Saunders CJ, et al. (2012) Rapid whole-genome sequencing for genetic disease diagnosis in neonatal intensive care units. *Sci Transl Med* 4(154):154ra135.
33. Talkowski ME, et al. (2012) Clinical diagnosis by whole-genome sequencing of a prenatal sample. *N Engl J Med* 367(23):2226–2232.
34. Dewey FE, et al. (2014) Clinical interpretation and implications of whole-genome sequencing. *JAMA* 311(10):1035–1045.
35. Miller NA, et al. (2015) A 26-hour system of highly sensitive whole genome sequencing for emergency management of genetic diseases. *Genome Med* 7(1):100.
36. Rehm HL, et al.; Working Group of the American College of Medical Genetics and Genomics Laboratory Quality Assurance Commitee (2013) ACMG clinical laboratory standards for next-generation sequencing. *Genet Med* 15(9):733–747.
37. Directors ABO; ACMG Board of Directors (2015) ACMG policy statement: Updated recommendations regarding analysis and reporting of secondary findings in clinical genome-scale sequencing. *Genet Med* 17(1):68–69.
38. Hehir-Kwa JY, et al. (2015) Towards a European consensus for reporting incidental findings during clinical NGS testing. *Eur J Hum Genet* 23(12):1601–1606.
39. Shah SH, et al. (2016) Opportunities for the cardiovascular community in the Precision Medicine Initiative. *Circulation* 133(2):226–231.
40. Reumers J, et al. (2011) Optimized filtering reduces the error rate in detecting genomic variants by short-read sequencing. *Nat Biotechnol* 30(1):61–68.
41. Raczy C, et al. (2013) Isaac: Ultra-fast whole-genome secondary analysis on Illumina sequencing platforms. *Bioinformatics* 29(16):2041–2043.
42. McKenna A, et al. (2010) The genome analysis toolkit: A MapReduce framework for analyzing next-generation DNA sequencing data. *Genome Res* 20(9):1297–1303.
43. Bentley DR, et al. (2008) Accurate whole human genome sequencing using reversible terminator chemistry. *Nature* 456(7218):53–59.
44. Wang K, Li M, Hakonarson H (2010) ANNOVAR: Functional annotation of genetic variants from high-throughput sequencing data. *Nucleic Acids Res* 38(16):e164.
45. Reese MG, Eeckman FH, Kulp D, Haussler D (1997) Improved splice site detection in Genie. *J Comput Biol* 4(3):311–323.
46. Dogan RI, Getoor L, Wilbur WJ, Mount SM (2007) SplicePort–an interactive splice-site analysis tool. *Nucleic Acids Res* 35(Web Server issue):W285–91.
47. Boyle AP, et al. (2012) Annotation of functional variation in personal genomes using RegulomeDB. *Genome Res* 22(9):1790–1797.
48. Wang H-Q, et al. (2012) Involvement of JNK and NF-κB pathways in lipopolysaccharide (LPS)-induced BAG3 expression in human monocytic cells. *Exp Cell Res* 318(1):16–24.
49. Whitfield TW, et al. (2012) Functional analysis of transcription factor binding sites in human promoters. *Genome Biol* 13(9):R50.
50. Raivich G, Behrens A (2006) Role of the AP-1 transcription factor c-Jun in developing, adult and injured brain. *Prog Neurobiol* 78(6):347–363.
51. Hess J, Angel P, Schorpp-Kistner M (2004) AP-1 subunits: Quarrel and harmony among siblings. *J Cell Sci* 117(Pt 25):5965–5973.
52. Kahlig KM, et al. (2014) Ranolazine reduces neuronal excitability by interacting with inactivated states of brain sodium channels. *Mol Pharmacol* 85(1):162–174.
53. Rajamani S, El-Bizri N, Shryock JC, Makielski JC, Belardinelli L (2009) Use-dependent block of cardiac late Na(+) current by ranolazine. *Heart Rhythm* 6(11):1625–1631.
54. Ginestet C (2011) ggplot2: Elegant graphics for data analysis. *J R Stat Soc Ser A Stat Soc* 174(1):245–246.
55. Mayo P, Hartshorne T, Li K (2010) CNV analysis using TaqMan copy number assays. *Curr Protoc Hum Genet* Chapter 2: Unit 2.13.
56. Vetter FJ, McCulloch AD (1998) Three-dimensional analysis of regional cardiac function: A model of rabbit ventricular anatomy. *Prog Biophys Mol Biol* 69(2-3):157–183.
57. Boyle PM, Deo M, Plank G, Vigmond EJ (2010) Purkinje-mediated effects in the response of quiescent ventricles to defibrillation shocks. *Ann Biomed Eng* 38(2):456–468.
58. O'Hara T, Virág L, Varró A, Rudy Y (2011) Simulation of the undiseased human cardiac ventricular action potential: Model formulation and experimental validation. *PLOS Comput Biol* 7(5):e1002061.
59. Ten Tusscher KH, Noble D, Noble PJ, Panfilov AV (2004) A model for human ventricular tissue. *Am J Physiol Heart Circ Physiol* 286(4):H1573–89.
60. Sampson KJ, Iyer V, Marks AR, Kass RS (2010) A computational model of Purkinje fibre single cell electrophysiology: Implications for the long QT syndrome. *J Physiol* 588(Pt 14):2643–2655.
61. Vigmond EJ, Aguel F, Trayanova NA (2002) Computational techniques for solving the bidomain equations in three dimensions. *IEEE Trans Biomed Eng* 49(11):1260–1269.
62. Vigmond EJ, Hughes M, Plank G, Leon LJ (2003) Computational tools for modeling electrical activity in cardiac tissue. *J Electrocardiol* 36(Suppl):69–74.
63. Plank G, et al. (2008) From mitochondrial ion channels to arrhythmias in the heart: Computational techniques to bridge the spatio-temporal scales. *Philos Trans A Math Phys Eng Sci* 366(1879):3381–3409.
64. Pahlajani DB, Miller RA, Serratto M (1975) Patterns of atrioventricular conduction in children. *Am Heart J* 90(2):165–171.
65. Schwartz PJ, et al.; European Society of Cardiology (2002) Guidelines for the interpretation of the neonatal electrocardiogram. A task force of the European Society of Cardiology. *Eur Heart J* 23(17):1329–1344.
66. Boyle PM, Williams JC, Ambrosi CM, Entcheva E, Trayanova NA (2013) A comprehensive multiscale framework for simulating optogenetics in the heart. *Nat Commun* 4:2370.
67. Silvetti MS, Drago F, Ravà L (2010) Determinants of early dilated cardiomyopathy in neonates with congenital complete atrioventricular block. *Europace* 12(9):1316–1321.
68. Dewey FE, et al. (2015) Sequence to medical phenotypes: A framework for interpretation of human whole genome DNA sequence data. *PLoS Genet* 11(10):e1005496.